Bioresource Technology 198 (2015) 488–496

Contents lists available at ScienceDirect

Bioresource Technology

journal homepage: www.elsevier.com/locate/biortech

A process for energy-efficient high-solids fed-batch enzymatic liquefaction of cellulosic biomass

M.J. Cardona [a], E.J. Tozzi [b], N. Karuna [c], T. Jeoh [c,*], R.L. Powell [a,d], M.J. McCarthy [c,d]

[a] Department of Chemical Engineering and Materials Science, University of California, Davis, One Shields Ave, Davis, CA 95616, USA
[b] Aspect Imaging, One Shields Ave, Davis, CA 95616, USA
[c] Department of Biological and Agricultural Engineering, University of California, Davis, One Shields Ave, Davis, CA 95616, USA
[d] Department of Food Science and Technology, University of California, Davis, One Shields Ave, Davis, CA 95616, USA

HIGHLIGHTS

- A fed-batch process for liquefaction was designed to enable high solids hydrolysis.
- Yield stress was used as a process control variable to optimize biomass additions.
- Upper limit of solids loading was ultimately limited by end-product inhibition.
- Enzyme addition schemes impact liquefaction rates and efficiency, and conversion.

ARTICLE INFO

Article history:
Received 5 July 2015
Received in revised form 4 September 2015
Accepted 5 September 2015
Available online 21 September 2015

Keywords:
Fed-batch
Enzymatic hydrolysis
Liquefaction
Rheology
Magnetic resonance imaging

ABSTRACT

The enzymatic hydrolysis of cellulosic biomass is a key step in the biochemical production of fuels and chemicals. Economically feasible large-scale implementation of the process requires operation at high solids loadings, i.e., biomass concentrations >15% (w/w). At increasing solids loadings, however, biomass forms a high viscosity slurry that becomes increasingly challenging to mix and severely mass transfer limited, which limits further addition of solids. To overcome these limitations, we developed a fed-batch process controlled by the yield stress and its changes during liquefaction of the reaction mixture. The process control relies on an in-line, non-invasive magnetic resonance imaging (MRI) rheometer to monitor real-time evolution of yield stress during liquefaction. Additionally, we demonstrate that timing of enzyme addition relative to biomass addition influences process efficiency, and the upper limit of solids loading is ultimately limited by end-product inhibition as soluble glucose and cellobiose accumulate in the liquid phase.

1. Introduction

Increasing global demand for energy has driven efforts toward developing forms of alternative energy that do not exhaust the limited resources available. Lignocellulosic biomass, abundant as an agricultural residue, is a rich source of sugars and other organic compounds that can be extracted for further processing into fuels (such as ethanol) and other value-added chemicals, and is thus a promising source of energy. One pathway to access the structural sugars is the enzymatic hydrolysis of biomass that typically follows thermochemical pretreatment to reduce biomass recalcitrance. Cellulases saccharify the pretreated biomass to its component sugars, which are converted downstream to the target bio-products. However, scale-up of cellulose saccharification can quickly become costly (Humbird et al., 2010, 2011). A potential route to lower process costs is to perform the hydrolysis step at high solids loadings of biomass (>15% (w/w)) to lower water use while increasing the concentrations of desired chemicals in product streams. High solids processing, however, introduces mixing and pumping challenges due to the low availability of free water (Cannella and Jørgensen, 2014; Koppram et al., 2014; Modenbach and Nokes, 2013) which leads to inefficient mass and heat transfer in the reactions. Moreover, high solids biomass hydrolysis may require more specialized equipment like scraped-surface reactors and roller bottle reactors, which may be limited in capacity and can add to the overall cost of the process (Di Risio et al., 2011; Larsen et al., 2012; Roche et al., 2009).

* Corresponding author. Tel.: +1 (530) 752 1020.
E-mail address: tjeoh@ucdavis.edu (T. Jeoh).

http://dx.doi.org/10.1016/j.biortech.2015.09.042
0960-8524/

Biomass saccharification in fed-batch mode has been shown to be a viable means for hydrolysis at high solids loadings (Modenbach and Nokes, 2013; Rosgaard et al., 2007). Fed-batch hydrolysis has been demonstrated using a variety of substrates including pretreated corn stover (Chandra et al., 2011; Hodge et al., 2009), sugarcane bagasse (Gao et al., 2014), and paper (Elliston et al., 2013); Elliston et al. achieved up to 65% (w/v) solids loading in a modified Simultaneous Saccharification and Fermentation (SSF) process (Elliston et al., 2013). By adding the substrate in batches, the enzymes are given time to liquefy the biomass to release water for the reaction and reduce particle size before more biomass is added. Batch additions of the substrate are typically done at regular time intervals. In one example, batch addition timing was optimized to maximize sugar yields (Gao et al., 2014), which required significant preliminary work to successfully optimize. A potential improvement over timed additions of fixed amounts of substrate (e.g., 6% solids added every 12 h) is to control both the timing and biomass quantity based on the rheology of the reaction mixture to tailor the process to minimize overall reaction time and mixing energy.

Rheology monitoring during fed-batch hydrolysis provides a way to adjust the process in real time so that batch additions are fully optimized. Viscosity is a readily measurable bulk-scale variable during enzymatic hydrolysis, and a means to optimize the size and timing of batch additions *in situ*. In a hydrolysis reaction, viscosity of the biomass slurry reduces rapidly to liquefy the reaction mixture due to endoglucanase activity (Skovgaard et al., 2014; Szijártó et al., 2011; Tozzi et al., 2014). Upon liquefaction, more free water is available in the bulk, which allows for more biomass solids to be added to achieve a higher total solids content. In fed-batch mode, higher solids content can be reached by adding more biomass upon liquefaction. Park et al. performed fed-batch hydrolysis using apparent viscosity (as a function of solids loading) as a control variable, and Sjoede et al. have patented a continuous process in which viscosity is continuously monitored off-line by sampling (Park et al., 2001; Sjoede et al., 2013); such approaches readily allow increasing solids to be added more efficiently, as additions are process-dependent and based on reaction feedback. However, these processes rely on off-line rheology measurements that are cumbersome, time-consuming and do not provide real-time feedback on the process.

We have improved the efficiency of fed-batch saccharification processes by using magnetic resonance imaging (MRI) rheometry of flowing slurries to measure on-going changes in viscosity and yield stress of biomass to obtain time-resolved rheological data during liquefaction (Lavenson et al., 2011; Skovgaard et al., 2014; Tozzi et al., 2014). We implemented this technique in hydrolysis experiments in fed-batch mode where *in situ* monitoring of yield stress was used as the control variable to determine the timing and amount of each batch addition. Liquefaction of biomass during enzymatic hydrolysis decreased slurry viscosity to reach a pseudo steady state (Skovgaard et al., 2014; Tozzi et al., 2014), signaling no further significant change in viscosity due to enzyme action, and that the biomass slurry is primed for further additions to reach higher solids contents. Thus, we used the onset of the steady state regime following liquefaction as the indicator for subsequent batch additions. We present results demonstrating the efficacy of yield stress controlled fed-batch hydrolysis of cellulosic biomass. We further explored the effects of timing of enzyme additions as differences have been observed in the past in total sugar released if all enzyme is added at the beginning versus in batches (Gao et al., 2014; Rosgaard et al., 2007). Likewise, timing of enzyme addition may have scale-up implications for further process optimization, thus we also investigated its impact on overall liquefaction extent and efficiency.

2. Methods

2.1. Experimental setup

Enzymatic hydrolysis experiments were performed in a 10 L recycle reactor connected to a continuous flow loop as previously described (Lavenson et al., 2011; Tozzi et al., 2014) to allow for instantaneous acquisition of rheological data during liquefaction. A 50 mM sodium citrate buffer at pH 5.0 was added to the stainless steel tank feeding into the flow loop and was allowed to circulate to reach reaction temperature (50 °C). A constant temperature was maintained by a heat exchanger in the flow loop; the heat exchanger consisted of a five-turn stainless steel coil submerged in a 23 L thermostatic water bath (PolyScience 9610, Niles, IL). In-line temperature was also continuously monitored with a type K thermocouple to ensure isothermal conditions. Once the buffer was pre-heated, cellulosic fibers (Solka-Floc, International Fiber Corporation, Tonawanda, NY), and a commercial cellulase mixture (Cellic CTec2, Novozymes A/S, Bagsvaerd, Denmark) were fed into the flow loop in a fed-batch manner. Amounts and concentrations added are detailed in Tables 2 and 3. Samples of 15 ml were taken periodically from the feed tank for sugar and total solids analyses.

2.2. Magnetic resonance imaging (MRI) for rheological measurements

In-line rheological measurements (Maneval et al., 1996; McCarthy et al., 1992; Powell et al., 1994) during hydrolysis were performed *in situ* and non-invasively using an in-line magnetic resonance imaging (MRI) flow loop as previously demonstrated (Lavenson et al., 2011; Skovgaard et al., 2014; Tozzi et al., 2014). An Aspect Imaging 1.03 T permanent magnet with a 0.3 T/m peak gradient strength (Aspect Imaging, Hevel Modi'in Industrial Area, Shoham, Israel) was used to obtain all images used in rheological analyses. The radio frequency coil encasing the imaging section of the pipe was a solenoid with three turns enclosing a volume 38 mm in diameter and 36 mm long. Velocity profiles as a function of radial position of the flowing biomass slurries were obtained throughout all experiments using a Pulsed Gradient Spin Echo (PGSE) sequence (Maneval et al., 1996; Powell et al., 1994). These velocity profiles, in conjunction with in-line differential pressure measurements, were used to obtain yield stresses during hydrolysis as shown in Tozzi et al. and Skovgaard et al. (Skovgaard et al., 2014; Tozzi et al., 2014). Yield stresses were thus measured instantaneously and used for process control in the fed-batch setups detailed in Section 2.4.

2.3. Cellulosic substrates

Two commercial delignified cellulosic fibers (Solka-Floc C100 and 200EZ) were used. Solka-Floc C100 and 200EZ mainly differed in their mean fiber length; C100 fibers are longer (mean fiber length: 0.444 mm) than 200EZ fibers (mean fiber length: 0.331 mm), and were otherwise similar in composition (Tozzi et al., 2014). The solids content of the fibers was measured using a Mettler-Toledo Halogen Moisture Analyzer (model HR83, Mettler-Toledo International, Inc., Columbus, OH) and determined to be 7.28% (w/w) and 7.44% (w/w) for C100 and 200EZ fibers, respectively. Compositions of the fibers were determined as per National Renewable Energy Laboratory Analytical Procedures (NREL LAP) (Hames et al., 2008; Sluiter et al., 2005, 2008) and are shown in Table 1.

Table 1
Compositional analysis of Solka-Floc fibers used. The compositional analysis was performed according to Hames et al. (2008) and Sluiter et al. (2005, 2008). Errors are from the standard error of triplicates.

Property	Solka-Floc 200EZ	Solka-Floc C100
Moisture content (% w.b.)	7.44	7.28
Mean length (length-weighted) (mm)	0.331	0.444
Glucan (% d.b.)	67.7 ± 8.7	71.5 ± 1.2
Xylan (% d.b.)	7.3 ± 0.8	7.1 ± 0.10
Mannan (% d.b.)	5.1 ± 0.10	4.3 ± 0.5
Acid insoluble lignin (% d.b.)	2.6 ± 0.4	3.0 ± 0.4

2.4. Fed-batch process control

Cellulosic fibers and cellulase enzymes were added to the recycle reactor in fed-batch mode. Yield stresses and in-line differential pressures of the biomass slurry were continuously measured, and these measurements were, in turn, used to decide when each batch addition was made. Fig. 1 depicts this decision-making scheme.

Prior to any biomass addition, 50 mM sodium citrate buffer was heated to the reaction temperature of 50 °C, at which point the first biomass addition was made. Biomass was added until the yield stress reached or exceeded 15 Pa and 100 Pa for Solka-Floc C100 and 200EZ fibers, respectively. These yield stress maxima were based on equipment used and differ between fiber sources because the differences in fiber lengths affect their crowding behavior (Tozzi et al., 2014). In other words, the longer C100 fibers behaved as a high consistency slurry at lower solids loadings than 200EZ fibers, which resulted in less C100 fibers added, comparatively, and therefore a lower yield stress (15 Pa) at the start of the experiment. Once the yield stress maximum was reached, Cellic CTec2 cellulases were added. The biomass was allowed to liquefy until the yield stress reached a low steady state value, at which point more biomass was added to reach the maximum yield stress again. If all enzymes were not added at the beginning of the trial, additional enzymes were also added at the point of biomass additions so as to maintain a constant enzyme-to-substrate ratio (5 FPU/g-biomass). This process was repeated for 12 h of hydrolysis. Tables 2 and 3 show the batch additions made during all fed-batch experiments. Table 2 shows additions for the experiment performed with Solka-Floc 200EZ (shorter fibers) to demonstrate the total solids achievable in this setup when all the enzyme is added at the beginning. Table 3 shows additions using Solka-Floc C100 (longer fibers) as a substrate, showing two modes of enzyme addition: one in which enzymes were added with each batch addition of biomass maintaining constant enzyme-to-substrate ratio (ENZ_B), and one in which the same total amount of enzyme was added at the start of hydrolysis (i.e., after the first biomass addition, ENZ_0). In other words, the experiments in Tables 3A and 3B have the same total amount of biomass and enzymes added, with the only difference being in the timing of enzyme additions.

It is worth noting that in the experiment wherein all the enzyme was added at the beginning (Tables 2 and 3B), the enzyme loading as a function of biomass content (i.e. FPU/g-biomass) did not remain constant throughout the reaction, and changed with each batch addition of biomass. After the last biomass addition, both trials had an effective enzyme loading of 5 FPU/g-biomass. The enzyme loading at each biomass content is included in Tables 2 and 3.

The apparent rate of liquefaction was determined from empirical fits to exponential decays in Fig. 4,

$$\tau_0 = a * e^{-b*t} \quad (1)$$

where τ_0 is the yield stress (Pa), t is time (h), a and b are fitting constants, and an initial rate of liquefaction is given by the derivative of Eq. (1) evaluated at $t = 0$ h, normalized for the start of each batch (i.e., time of batch addition). These fits are not meant as a universal model for liquefaction, but rather as an empirical tool for comparison between trials.

2.5. Analysis of samples

Samples were periodically taken from the feed tank during experiments to measure total solids contents and soluble sugar concentrations. These measurements were used to determine glucan conversion over the course of hydrolysis. Hydrolysis was stopped prior to measurements by quenching in a water bath at 80 °C for 10 min.

2.5.1. Total solids measurements

Total solids fractions were measured using both a Halogen Mettler Toledo Moisture Analyzer (model HR83, Mettler-Toledo

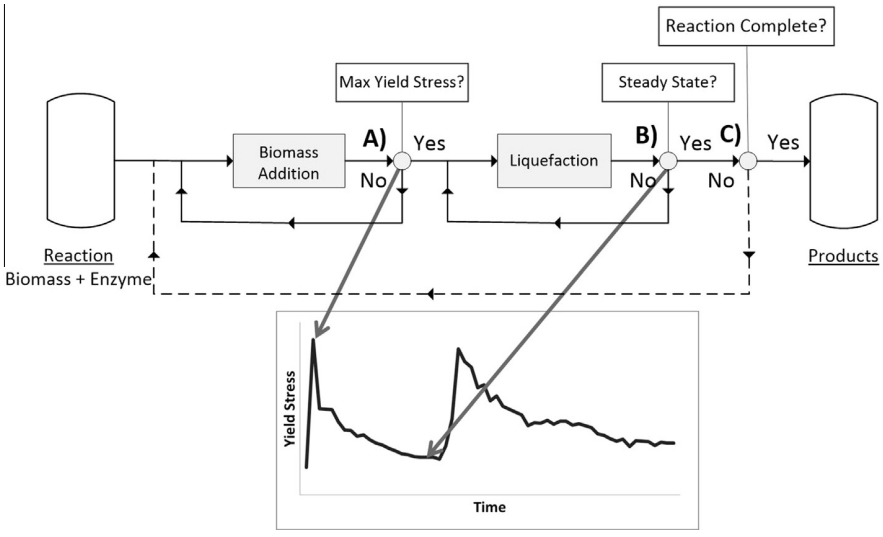

Fig. 1. Fed-batch process control scheme. (A) Biomass additions were made until the yield stress reached a predetermined maximum, at which point the slurry was allowed to liquefy by enzymatic action. (B) Once yield stress reached a low steady state value, another biomass addition was made. The amount added was again dependent on the amount of biomass necessary to reach the maximum yield stress. (C) Additions continued thusly for the duration of the experiments.

Table 2
Fed-batch experimental setup. Biomass, buffer, and enzyme additions made for experiments with Solka-Floc 200EZ with all enzymes added initially.

Solka-Floc 200EZ	Batch addition								
	1	2	3	4	5	6	7	8	9
Hydrolysis time (h)	0.00	0.20	0.75	1.25	2.33	3.75	4.92	7.75	11.75
Total solids (%(w/w))	16.88	20.76	22.91	24.51	26.01	26.74	28.23	29.51	30.71
Reactor contents									
Buffer added (L)	5.3	0.0	0.0	0.0	0.0	0.0	0.0	0.0	0.0
Biomass added (kg)	1.200	0.356	0.213	0.168	0.165	0.083	0.174	0.157	0.154
Total biomass in reactor (kg)	1.200	1.556	1.769	1.938	2.103	2.186	2.360	2.517	2.671
Enzyme added (ml)	160	0	0	0	0	0	0	0	0
Effective enzyme loading (FPU/g-biomass)	9.53	7.35	6.46	5.90	5.44	5.23	4.85	4.54	4.28

Table 3
Fed-batch experimental setup for ENZ_B and ENZ_0. Biomass, buffer, and enzyme additions made for experiments with Solka-Floc C100 with enzymes added in a batchwise manner (ENZ_B) (A), and with all enzymes added initially (ENZ_0) (B).

Solka-Floc C100	Batch addition					
A. ENZ_B	1	2	3	4	5	6
Hydrolysis time (h)	0.00	0.52	1.25	2.37	4.23	6.55
Total solids (%(w/w))	8.77	10.94	13.00	15.37	17.30	19.28
Reactor contents						
Buffer added (L)	6.5	0.0	0.0	0.0	0.0	0.0
Biomass added (kg)	0.677	0.192	0.193	0.236	0.204	0.223
Total biomass in reactor (kg)	0.677	0.869	1.063	1.299	1.502	1.725
Enzyme added (ml)	47	13	14	17	14	16
Effective enzyme loading (FPU/g-biomass)	5.00	5.00	5.00	5.00	5.00	5.00
	Batch addition					
B. ENZ_0	1	2	3	4	5	6
Hydrolysis time (h)	0.00	0.28	0.77	1.53	2.70	4.18
Total solids (%(w/w))	8.66	10.83	12.89	15.29	17.25	19.28
Reactor contents						
Buffer added (L)	6.5	0.0	0.0	0.0	0.0	0.0
Biomass added (kg)	0.677	0.192	0.193	0.236	0.204	0.223
Total biomass in reactor (kg)	0.677	0.869	1.061	1.298	1.502	1.725
Enzyme added (ml)	121	0	0	0	0	0
Effective enzyme loading (FPU/g-biomass)	12.78	9.96	8.15	6.67	5.76	5.01

International, Inc., Columbus, OH) and a vacuum oven drying method as shown by Weiss et al. (2010). In the Moisture Analyzer, samples were heated to 105 °C until there was less than a 0.05% change in the weight of the sample, at which point the total solids fraction was determined based on the weight of water that evaporated.

2.5.2. Sugar content measurement by high-performance liquid chromatography (HPLC)

Hydrolyzate samples taken periodically from the flow loop return line were analyzed for soluble sugars by high-performance liquid chromatography (HPLC, Shimadzu Scientific Instruments, Columbia, MD). Separation was carried out on an Aminex HPX-87P column with de-ashing and Carbo-P guard cartridges (BioRad, Hercules, CA) and sugar concentrations were measured by refractive index. The flow rate was 0.6 ml/min at 80 °C using nanopure water as the mobile phase. Calibration was performed with standard solutions of D-glucose, L-arabinose, D-xylose, D-mannose, D-galactose and D-cellobiose.

2.5.3. Glucan conversion in high solids fed-batch hydrolysis

Glucose yields were determined as per Zhu et al. (2011), which was found fit for calculating yields due to the experiment being performed at high solids loadings, in which the density of the liquid phase and the liquid volume in the reactor would be changing during the reaction. Glucose yields were calculated as follows,

$$Y_g = \frac{C_g * V_h - C_{g,0} * V_{h,0}}{\varphi_G * W_t * f_{ts,0} * X_{is,0} + \varphi_{gos} * C_{gos,0} * V_{h,0}}, \quad (2)$$

where Y_g is the glucose yield (as a fraction of 100), C_g and $C_{g,0}$ are concentrations of glucose (g/L), V_h and V_{h0}, are volumes of the hydrolyzate (L), φ_G is the molecular weight ratio of glucose to glucan monomer (1.11), W_t is the total weight of the hydrolysis assay (g), $f_{ts,0}$ is the initial mass fraction of total solids, $X_{is,0}$ is the initial mass fraction of insoluble solids in total solids (i.e., $f_{is,0}/f_{ts,0}$), φ_{gos} is the molecular weight ratio of glucose to average monomer weight of glucose oligomers (1.08), and $C_{gos,0}$ is the initial concentration of glucose oligomers (Zhu et al., 2011). All terms in Eq. (2) with subscript "0" correspond to initial values; these changed with each batch addition and thus all reported glucose yields account for the changing amount of biomass in the reactor. The fraction of insoluble solids ($f_{is,0}$) was calculated based on the measured fraction of total solids ($f_{ts,0}$) and by using the method detailed by Weiss et al. (2010). Eq. (3) details how it was calculated,

$$f_{is} = \frac{f_{ts} - y_{ss}}{1 - y_{ss}}, \quad (3)$$

where y_{ss} is the fraction component of soluble solids in the liquid of the slurry, or m_{ss}/m_l (dimensionless), and m_{ss} is the total mass of soluble solids (g, as determined by HPLC) and m_l is the total mass of liquid in the slurry (g). Total solids and sugar concentration

measurements were thus used to obtain glucose yields during high solids fed-batch hydrolysis.

3. Results and discussion

3.1. Monitoring yield stress as a control variable to determine fed-batch addition and timing

Yield stress was used as a process control variable during 12 h of hydrolysis of Solka-Floc 200EZ (Fig. 2). Continuous monitoring of the suspension yield stress during the reaction provided a means to control the amount of biomass in each batch and the timing of the batch additions. The maximum amount of biomass that could be added at the start of the reaction and at each batch addition was limited by the maximum allowable yield stress of the flow loop equipment of 100 Pa. Following each batch addition, as the enzymes liquefied the substrate, the suspension yield stress dropped to a steady state indicating that the biomass slurry was able to contain more solids due to the increase in the availability of water in the bulk. Thus, the timing of subsequent batch additions was determined by the onset of this steady state. In the first few batch additions, liquefaction occurred very rapidly as indicated by precipitous drops in the suspension yield stress immediately following substrate addition (Fig. 2). By the fifth batch addition (hexagons in Fig. 2), a noticeable decrease in liquefaction rates was observed. With this fed-batch processing scheme, we increased total solids loading in the reaction from 16.9% (w/w) solids to 30.7% (w/w) solids over the 12 h duration.

Despite the continuous addition of fresh enzymes with each batch of substrate, glucan conversion slowed down rapidly within the first 2 h of hydrolysis and tapered off at approximately 50% by the end of the 12 h reaction time. A relatively low overall enzyme loading was used (5 FPU/g-biomass), and glucan conversion was computed only from glucose and cellobiose release, which were the primary products of interest. Although glucose was the dominant contributor to glucan conversion (Fig. 3A), a continuous increase in cellobiose concentration was observed as hydrolysis progressed. The accumulation of cellobiose strongly indicates end-product inhibition of β-glucosidases in the system. The glucose inhibition constant (K_I) for β-glucosidase ranges from 0.04 to 6 g/L on cellobiose (Andrić et al., 2010). Glucose concentrations surpass these values within the first few minutes of hydrolysis (22.6 g/L by 5 min of hydrolysis, Fig. 3A). In addition, the cellobiose inhibition constant K_I for crude *Trichoderma reesei* cellulases on Solka-Floc has been reported as 2.3 g/L (Asenjo, 1983). This concentration is exceeded after the third batch addition (5.1 g/L by 1 h, Fig. 3B), indicating that cellobiohydrolases are likely also inhibited. It is possible that cello-oligosaccharides were also accumulating during hydrolysis, but we did not measure these concentrations. Higher glucan conversions are likely achievable if end-products are separated and removed from the hydrolyzate.

The data in Fig. 2 demonstrate the feasibility of achieving higher solids loadings in the saccharification reaction with minimal increase in mixing energy and without needing specialized

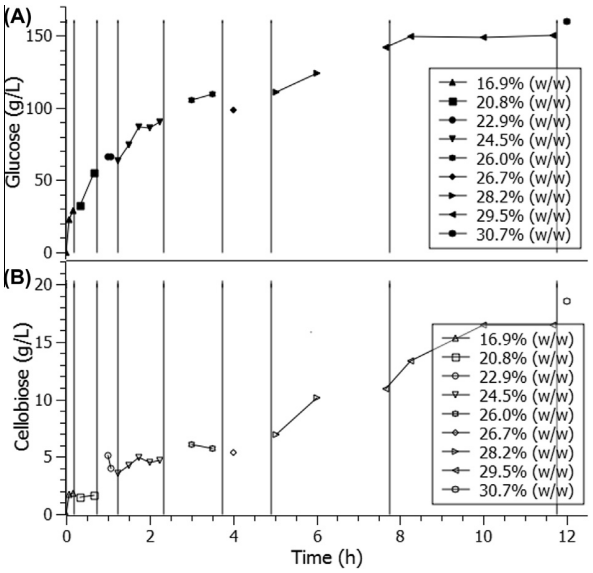

Fig. 3. End-product inhibition during fed-batch hydrolysis of Solka-Floc. Glucose (A) and cellobiose (B) concentrations released during hydrolysis of Solka-Floc 200EZ in fed-batch mode. Similar symbols indicate similar solids loadings. Lines are included to guide the eye. Vertical lines indicate when batch additions of biomass were made.

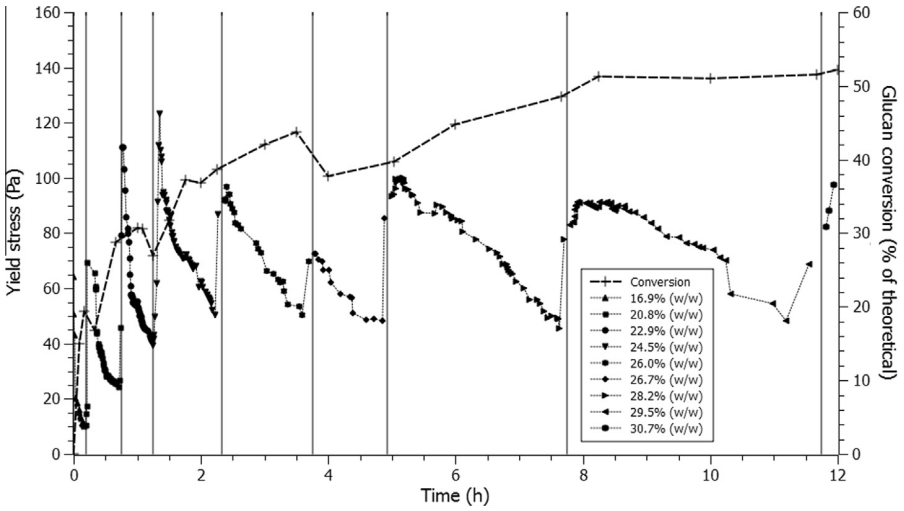

Fig. 2. Fed-batch hydrolysis of Solka-Floc. Yield stress and glucan conversion as a function of hydrolysis time of Solka-Floc 200EZ in fed-batch mode. Symbol changes indicate a change (i.e., increase) in total solids loading due to a batch addition. Vertical lines indicate when batch additions of biomass were made. Spikes in yield stress occurred immediately following batch additions of biomass. Superimposed, glucan conversion as a function of hydrolysis time is shown (crosses, secondary vertical axis). Lines are included to guide the eye.

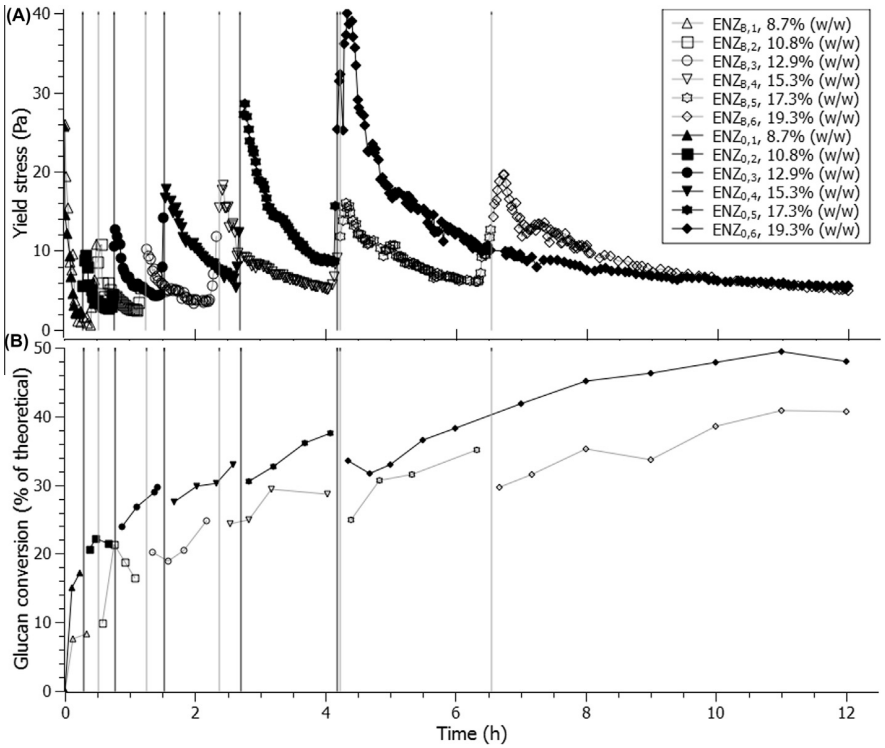

Fig. 4. Different modes of enzyme addition during fed-batch hydrolysis of Solka-Floc. Yield stress (A) and glucan conversion (B) as a function of hydrolysis time of Solka-Floc C100 in fed-batch mode. Similar symbols indicate similar total solids loadings (in both trials), and symbol changes indicate a change (i.e., increase) in total solids loading within a trial due to a batch addition. Empty symbols indicate that cellulases were added with each batch addition of biomass (ENZ_B) and filled-in symbols indicate that all cellulases were added initially (ENZ_0). Spikes in yield stress occurred during batch additions of biomass. Lines joining data points are included to guide the eye. Vertical lines indicate when batch additions were made. Gray lines correspond to ENZ_B and black correspond to ENZ_0.

equipment such as scraped-surface reactors. We found the same results using longer cellulosic fibers, Solka-Floc C100 (Fig. 4). The two Solka-Floc substrates, 200EZ and C100, are compositionally similar but differences in their aspect ratios affect fiber crowding behavior and thereby the rheology of the fiber suspensions (Tozzi et al., 2014). As with the fed-batch operation using 200EZ, the maximum mass of C100 that could be added with each batch depended on the capability of both the system and the biomass slurry to take on additional solids that was assessed by monitoring the yield stress of the reaction. As noted previously in (Tozzi et al., 2014), the longer fibers of C100 increases fiber–fiber interactions (higher crowding numbers) thereby reaching greater yield stress in the slurry at lower solids loadings. Relying on concentrations is therefore not an effective means to determine batch additions in fed-batch mode. Rather, suspension yield stress is a more effective process control variable when working with morphologically heterogeneous substrates.

3.2. Timing of enzyme addition affects liquefaction rates

Fig. 4 compares two fed-batch hydrolysis reactions of Solka-Floc C100 under identical reaction conditions and biomass additions, but differing in the timing of the enzyme addition. In the 'ENZ_B' reaction, enzymes were added with each batch addition of substrate at a constant enzyme-to-substrate (E/S) ratio, while in the 'ENZ_0' reaction, the total amount of enzyme was added at the beginning of the experiment. The overall E/S ratio in the ENZ_B and ENZ_0 reactions were equivalent over the full course of the reactions (Table 3). The termination of the reaction at 12 h was based on the onset of the steady state in liquefaction after the last batch addition in the ENZ_B reaction.

Adding all the enzyme at the start of the hydrolysis reaction was beneficial for process efficiency as rapid liquefaction allowed earlier batch additions of substrate, thus achieving higher solids loadings faster (Fig. 4 and Table 3). It took 6.5 h to reach the final solids loading (19.3% (w/w)) in ENZ_B, whereas the same additions were completed by 4.5 h in ENZ_0. Initially, the E/S ratio was much higher in ENZ_0, as the enzyme loading was over double that of ENZ_B (12.8 vs. 5 FPU/g-biomass in the first batch, respectively), which is likely the reason for the more rapid decline in yield stress in ENZ_0. However, after the addition of batch 5, where E/S loadings in ENZ_0 and ENZ_B were more closely matched (5.76 FPU/g-biomass and 5 FPU/g-biomass, respectively), the biomass suspension yield stress in ENZ_0 took only approximately one hour to reach a steady state whereas it took nearly two hours in ENZ_B (stars in Fig. 4A). These observations suggest that while a higher E/S ratio may account for initial improvements, additional factors are at play to make liquefaction more efficient in the later additions for ENZ_0. Liquefaction of biomass is largely attributed to fiber shortening by endo-activity in the cellulase mixtures (Skovgaard et al., 2014; Tozzi et al., 2014). Moreover, endoglucanases have been shown to be resilient under high-shear conditions (Ye et al., 2012). Thus one possibility is that adding all the endo-acting enzymes at the beginning of the reaction gave more time for the full loading of endoglucanases to hydrolyze the substrate. Additionally, the longer exposure to the substrate added earlier in the reaction may allow for more release of constrained water, thus decreasing viscosities in the soluble phase and facilitating mass transfer of the same endoglucanases to biomass in subsequent additions (Roberts et al., 2011). The addition of new biomass to an ongoing biomass hydrolysis reaction (as in fed-batch mode) has been shown to adversely affect glucose yields (Rosgaard

et al., 2007), so it is not surprising that it would also affect other modes of enzyme action (e.g., viscosity reduction). Therefore, adding all the enzymes at the beginning may serve to counteract the inhibitory effects of new substrate additions by more thoroughly liquefying the first batches of substrate.

Estimates of the apparent initial rates of liquefaction following each batch addition show that ENZ_0 consistently liquefied at a faster rate than ENZ_B, even in later batch additions where effective enzyme loadings were similar (Fig. 6A). The rates of liquefaction for the first batch addition for both ENZ_0 and ENZ_B were much higher than the rest. This is consistent with prior observation that biomass additions may result in reduced enzyme activity due to insufficient reaction time to access the newer substrate (Rosgaard et al., 2007). Overall, adding all cellulases initially facilitated increasing higher solids faster due to improved liquefaction efficiency.

3.3. Timing of enzyme addition affects extent of saccharification

Adding all enzyme initially (ENZ_0) resulted in higher glucan conversions in every batch, especially in the first addition (17.2% versus 8.3% conversion for ENZ_0 and ENZ_B, respectively). However, starting from the third batch addition (downward triangles in Fig. 4B), the curves are equidistant, indicating that glucan conversions between the two modes of addition become offset by the same amount. Moreover, glucan conversions in both reactions slow down considerably and plateau at around 40% and 45% for ENZ_B and ENZ_0, respectively.

Glucose concentrations (Fig. 5A) continuously increased throughout hydrolysis, but plateaued for both ENZ_0 and ENZ_B during the last 4 h of hydrolysis. This plateau, just beyond 60 g/L glucose, may be due to end-product inhibition of β-glucosidases in the reaction. K_I for β-glucosidase ranges from 0.04 to 6 g/L on cellobiose, which is exceeded in the first 10 min of hydrolysis for both ENZ_B and ENZ_0 (Andrić et al., 2010). In both ENZ_0 and ENZ_B reactions, cellobiose concentrations increased following each batch addition before decreasing again, suggesting a lag in the β-glucosidase activity compared to cellobiohydrolase activity in the reactions. In addition, during the last batch addition for both ENZ_0 and ENZ_B (diamonds in Fig. 5B) cellobiose did not completely hydrolyze, but rather stabilized at a concentration of approximately 2 g/L. The plateau in glucose concentration coupled with the accumulation of cellobiose indicates end-product inhibition of β-glucosidases in the reaction. Moreover, the stabilization of the cellobiose concentration further suggests that the cellobiohydrolases are not actively hydrolyzing cellulose in the reactions. Overall, ENZ_0 yielded more glucose, but this was likely due to the initial "boost" during the first batch when the enzyme-to-substrate ratio was much higher, but saccharification becomes highly end-product inhibited regardless of mode of enzyme addition. Separation or fermentation of products in the hydrolyzate from the unhydrolyzed biomass slurry may help reach higher conversions than those seen in these studies by overcoming or reducing end-product inhibition altogether. For instance, by converting this fed-batch saccharification process into a Simultaneous Saccharification and Fermentation (SSF) process – where microorganisms that can ferment the sugar products are added to the same saccharification reactor – end products would be fermented, and end product accumulation and inhibition of cellulases would be avoided. Fed-batch SSF processes have been previously demonstrated (Elliston et al., 2013; Rudolf et al., 2005).

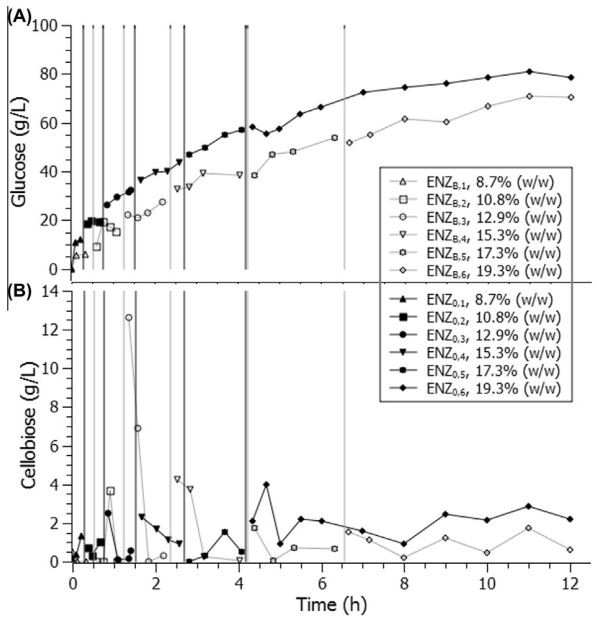

Fig. 5. End-product inhibition during fed-batch hydrolysis of Solka-Floc with different modes of enzyme addition. Glucose (A) and cellobiose (B) concentrations released during hydrolysis of Solka-Floc C100 in fed-batch mode. Similar symbols indicate similar solids loadings. Similar symbols indicate similar total solids loadings (in both trials), and symbol changes indicate a change (i.e., increase) in total solids loading within a trial due to a batch addition. Empty symbols indicate that cellulases were added with each batch addition of biomass (ENZ_B) and filled-in symbols indicate that all cellulases were added initially (ENZ_0). Lines joining data points are included to guide the eye. Vertical lines indicate when batch additions were made. Gray lines correspond to ENZ_B and black lines correspond to ENZ_0.

As glucan conversion only measures release of glucose and cellobiose, it is hard to say what other effects on saccharification the mode of enzyme addition has, or whether the high solids effects already mentioned (end-product inhibition, mass transfer limitations, high viscosities) affect the release of other components (e.g., pentoses, other oligosaccharides). The focus on glucan was due to the nature of the highly cellulosic composition of the substrate studied, but further research on the effects of enzyme addition on other physicochemical aspects of hydrolysis (e.g., particle size, oligosaccharide release and irreversibly bound enzyme concentrations) may provide more insight into kinetics at high solids. This is ultimately very desirable if scale-up at high solids contents is to be realized.

3.4. Timing of enzyme addition affects process and energy efficiency

Process efficiency is paramount when deciding processing parameters, and ultimately for successful scale-up. In both ENZ_B and ENZ_0 reactions, the same equipment and reaction conditions were used, with the only difference being the timing of enzyme and biomass additions. Everything else being equal, the timing of biomass additions ultimately came down to the liquefaction efficiency of each setup, which directly affected the pumping requirements for each process. Given the same pumping power, a more liquefied, less viscous slurry experiences less frictional losses (i.e., energy dissipation) than a more viscous slurry. Frictional losses can be represented by head losses, or pressure losses, which can be characterized by the Darcy–Weisbach equation (Eq. (4)),

$$h_f = f_D * \frac{L}{D} * \frac{\bar{V}^2}{2g}, \tag{4}$$

where the head loss due to frictional losses, h_f (m), is a function of the pipe dimensions (L, length (m), and D, inner diameter (m)), mean fluid velocity $\bar{V}$ (m/s), acceleration due to gravity, (m/s^2), and a dimensionless Darcy friction factor f_D, which is dependent on the Reynolds number of the fluid and pipe surface properties.

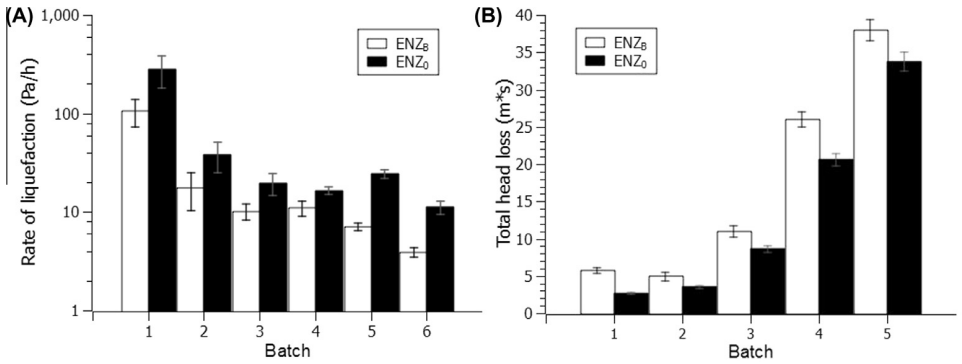

Fig. 6. Liquefaction efficiency depends on mode of enzyme addition. (A) Semi-log bar graph of rates of liquefaction (given as changes in yield stress over time) of both modes of enzyme addition (ENZ_B and ENZ_0, in white and black, respectively) for each batch addition. (B) Total head loss of both modes of enzyme addition (ENZ_B and ENZ_0, in white and black, respectively) for each batch addition. Error bars are from fitting confidence intervals (95%).

Head loss, with units of length, is defined as the rise in fluid level in a vertical column in the absence of frictional losses. While head loss can be readily calculated at individual points in time for which we have pressure drop, velocity, and composition data (i.e., for all points in Fig. 4), in order to compare the two enzyme addition schemes it is more relevant to calculate the total head loss during each batch. The total head (m * s) loss during a batch can be defined as the sum of instantaneous head losses (Eq. (5)),

$$Total\ head\ loss = \sum_i h_{f,i} * \Delta t, \tag{5}$$

where $h_{f,i}$ are instantaneous values of head loss, and Δt is time between head loss data points (i.e., the time between when $h_{f,i-1}$ and $h_{f,i}$ were obtained). Because head loss was determined at discrete points in time, a discrete sum was used to calculate total head loss. Fig. 6B shows what total head losses were for each batch, for both setups, using Eqs. (4) and (5).

It is worth noting that the last batch addition continued past the onset of steady state, and therefore took a significantly higher amount of time than the other batches; this resulted in the total head loss values for the sixth batch addition being significantly higher than the rest (results not shown). Fig. 6 shows that total head losses were consistently higher for ENZ_B than for ENZ_0, emphasizing again that adding all enzyme initially is desirable as it incurred lower energy losses. Lower head losses corresponded well with higher rates of liquefaction (Fig. 6A). From Eq. (5), it is evident that because ENZ_0 batches spanned less time than ENZ_B batches, total head loss per ENZ_0 batch is less than for the equivalent ENZ_B batch. Furthermore, the improved liquefaction in ENZ_0 resulted in slightly larger Reynolds numbers for the biomass slurry due to slightly higher mean velocities and lower viscosities. The friction factor f_D in Eq. (4) was calculated as $64/Re$ for laminar flow in circular pipes, which means lower head losses for fluids with higher Reynolds numbers in smooth-walled pipes.

It is important to account for energy usage and losses when evaluating process efficiency; determining pumping head loss can become of high value considering the difficulty of pumping biomass at high solids concentrations. By looking at the total head loss, as well as rates of liquefaction and saccharification, we were able to determine that adding all the enzyme initially resulted in a more efficient process to reach and process high solids contents.

This fed-batch process design can serve as a tool to study hydrolysis kinetics at high solids contents, varying substrates, enzyme activities and the timing of substrate and enzyme additions to provide deeper bulk-scale insights into the high solids effects during biomass saccharification. The current studies were done on delignified cellulosic fibers, and therefore results could be different on a lignocellulosic substrate due to compositional differences. However, initial studies on a model cellulosic substrate are still relevant to process scale-up. Past work on hydrothermally pretreated wheat straw, a substrate comprised of 29.5% lignin, also showed fast decays in viscosity during liquefaction (Skovgaard et al., 2014), indicating that a fed-batch setup that exploits liquefaction to get to higher solids contents could be used. Different enzyme feeding schemes in this process might help in improving saccharification rates on a lignocellulosic substrate. Saccharification is also significantly slower than liquefaction, thus with a lignocellulosic substrate, much longer hydrolysis times or higher enzyme loadings would be needed to improve on conversions seen here. Ultimately, altering modes of enzyme addition does have an impact on hydrolysis, and it provides an opportunity for process optimization.

4. Conclusion

A cellulosic substrate was hydrolyzed in fed-batch mode to easily attain high total solids loadings by using continuous monitoring of rheological changes in the biomass slurry. Adding all enzyme initially resulted in higher glucose yields and a more energy-efficient process due to faster liquefaction per batch and faster additions of solids. At high solids loadings, however, end-product inhibition becomes unavoidable without removal of products from the hydrolysate. Overall, the platform and process design presented here are a valuable means by which to further understand the high solids effects and hydrolysis kinetics at high solids loadings.

Acknowledgements

The authors would like to thank Novozymes A/S for samples of Cellic CTec 2 and the Center for Process Analysis and Control, University of Washington and the USDA National Institute of Food and Agriculture, Hatch project number 1001068 for partial funding of this work. We would also like to thank Scott Strobel and Akshata Mudinoor for help during experiments. The authors declare that they have no conflicts of interest related to the publication of this work.

Appendix A. Supplementary material

Supplementary data associated with this article can be found, in the online version, at http://dx.doi.org/10.1016/j.biortech.2015.09.042.

References

Andrić, P., Meyer, A.S., Jensen, P.A., Dam-Johansen, K., 2010. Reactor design for minimizing product inhibition during enzymatic lignocellulose hydrolysis: I. Significance and mechanism of cellobiose and glucose inhibition on cellulolytic enzymes. Biotechnol. Adv. 28, 308–324.

Asenjo, J.A., 1983. Maximizing the formation of glucose in the enzymatic hydrolysis of insoluble cellulose. Biotechnol. Bioeng. 25, 3185–3190.

Cannella, D., Jørgensen, H., 2014. Do new cellulolytic enzyme preparations affect the industrial strategies for high solids lignocellulosic ethanol production? Biotechnol. Bioeng. 111, 59–68.

Chandra, R.P., Au-Yeung, K., Chanis, C., Roos, A.A., Mabee, W., Chung, P.A., Ghatora, S., Saddler, J.N., 2011. The influence of pretreatment and enzyme loading on the effectiveness of batch and fed-batch hydrolysis of corn stover. Biotechnol. Prog. 27, 77–85.

Di Risio, S., Hu, C., Saville, B., Liao, D., Lortie, J., 2011. Large-scale, high-solids enzymatic hydrolysis of steam-exploded poplar. Biofuels Bioprod. Biorefin. 5, 609–620.

Elliston, A., Collins, S.R., Wilson, D.R., Roberts, I.N., Waldron, K.W., 2013. High concentrations of cellulosic ethanol achieved by fed batch semi simultaneous saccharification and fermentation of waste-paper. Bioresour. Technol. 134, 117–126.

Gao, Y., Xu, J., Yuan, Z., Zhang, Y., Liu, Y., Liang, C., 2014. Optimization of fed-batch enzymatic hydrolysis from alkali-pretreated sugarcane bagasse for high-concentration sugar production. Bioresour. Technol. 167, 41–45.

Hames, B., Ruiz, R., Scarlata, C., Sluiter, A., Sluiter, J., Templeton, D., 2008. Preparation of Samples for Compositional Analysis. Laboratory Analytical Procedure NREL/TP-510-42620. National Renewable Energy Laboratory.

Hodge, D.B., Karim, M.N., Schell, D.J., McMillan, J.D., 2009. Model-based fed-batch for high-solids enzymatic cellulose hydrolysis. Appl. Biochem. Biotechnol. 152, 88–107.

Humbird, D., Davis, R., Tao, L., Kinchin, C., Hsu, D., Aden, A., Schoen, P., Lukas, J., Olthof, B., Worley, M., 2011. Process Design and Economics for Biochemical Conversion of Lignocellulosic Biomass to Ethanol: Dilute-acid Pretreatment and Enzymatic Hydrolysis of Corn Stover. NREL/TP-5100-47764. National Renewable Energy Laboratory.

Humbird, D., Mohagheghi, A., Dowe, N., Schell, D.J., 2010. Economic impact of total solids loading on enzymatic hydrolysis of dilute acid pretreated corn stover. Biotechnol. Prog. 26, 1245–1251.

Koppram, R., Tomás-Pejó, E., Xiros, C., Olsson, L., 2014. Lignocellulosic ethanol production at high-gravity: challenges and perspectives. Trends Biotechnol. 32, 46–53.

Larsen, J., Haven, M.Ø., Thirup, L., 2012. Inbicon makes lignocellulosic ethanol a commercial reality. Biomass Bioenergy 46, 36–45.

Lavenson, D.M., Tozzi, E.J., McCarthy, M.J., Powell, R.L., 2011. Yield stress of pretreated corn stover suspensions using magnetic resonance imaging. Biotechnol. Bioeng. 108, 2312–2319.

Maneval, J.E., McCarthy, K.L., McCarthy, M.J., Powell, R.L. 1996. Nuclear Magnetic Resonance Imaging Rheometer, (Ed.) U.S.P.a.T. Office. United States Patent 5,532,593.

McCarthy, K.L., Kauten, R.J., Agemura, C.K., 1992. Application of NMR imaging to the study of velocity profiles during extrusion processing. Trends Food Sci. Technol. 3, 215–219.

Modenbach, A.A., Nokes, S.E., 2013. Enzymatic hydrolysis of biomass at high-solids loadings – a review. Biomass Bioenergy 56, 526–544.

Park, E.Y., Michinaka, A., Okuda, N., 2001. Enzymatic hydrolysis of waste office paper using viscosity as operating parameter. Biotechnol. Prog. 17, 379–382.

Powell, R.L., Maneval, J.E., Seymour, J.D., McCarthy, K.L., McCarthy, M.J., 1994. Note: Nuclear magnetic resonance imaging for viscosity measurements. J. Rheol. 38, 1465–1470.

Roberts, K.M., Lavenson, D.M., Tozzi, E.J., McCarthy, M.J., Jeoh, T., 2011. The effects of water interactions in cellulose suspensions on mass transfer and saccharification efficiency at high solids loadings. Cellulose 18, 759–773.

Roche, C.M., Dibble, C.J., Knutsen, J.S., Stickel, J.J., Liberatore, M.W., 2009. Particle concentration and yield stress of biomass slurries during enzymatic hydrolysis at high-solids loadings. Biotechnol. Bioeng. 104, 290–300.

Rosgaard, L., Andric, P., Dam-Johansen, K., Pedersen, S., Meyer, A.S., 2007. Effects of substrate loading on enzymatic hydrolysis and viscosity of pretreated barley straw. Appl. Biochem. Biotechnol. 143, 27–40.

Rudolf, A., Alkasrawi, M., Zacchi, G., Lidén, G., 2005. A comparison between batch and fed-batch simultaneous saccharification and fermentation of steam pretreated spruce. Enzym. Microb. Technol. 37, 195–204.

Sjoede, A., Froelander, A., Lersch, M., Roedsrud, G., Hals, K., Kloeften, A.M., Delin, L., Johansson, M.H., 2013. Enzymatic Hydrolysis of Cellulose, (Ed.) U.S.P.a.T. Office. United States Patent 20,130,217,074.

Skovgaard, P.A., Cardona, M., Tozzi, E., Siika-aho, M., Thygesen, L.G., Jeoh, T., McCarthy, M., Jørgensen, H., 2014. The role of endoglucanase and endoxylanase in liquefaction of hydrothermally pretreated wheat straw. Biotechnol. Prog. 30, 923–931.

Sluiter, A., Hames, B., Ruiz, R., Scarlata, C., Sluiter, J., Templeton, D. 2005. Determination of Ash in Biomass. Laboratory Analytical Procedure National Renewable Energy Laboratory.

Sluiter, A., Hames, B., Ruiz, R., Scarlata, C., Sluiter, J., Templeton, D., Crocker, D., 2008. Determination of Structural Carbohydrates and Lignin in Biomass. Laboratory Analytical Procedure, National Renewable Energy Laboratory.

Szijártó, N., Siika-Aho, M., Sontag-Strohm, T., Viikari, L., 2011. Liquefaction of hydrothermally pretreated wheat straw at high-solids content by purified Trichoderma enzymes. Bioresour. Technol. 102, 1968–1974.

Tozzi, E.J., Lavenson, D.M., Cardona, M., Karuna, N., Jeoh, T., McCarthy, M.J., Powell, R.L., 2014. Effect of fiber structure on yield stress during enzymatic conversion of cellulose. AIChE J. 60, 1582–1590.

Weiss, N.D., Stickel, J.J., Wolfe, J.L., Nguyen, Q.A., 2010. A simplified method for the measurement of insoluble solids in pretreated biomass slurries. Appl. Biochem. Biotechnol. 162, 975–987.

Ye, Z., Hatfield, K.M., Eric Berson, R., 2012. Deactivation of individual cellulase components. Bioresour. Technol. 106, 133–137.

Zhu, Y., Malten, M., Torry-Smith, M., McMillan, J.D., Stickel, J.J., 2011. Calculating sugar yields in high solids hydrolysis of biomass. Bioresour. Technol. 102, 2897–2903.